Clinical Pharmacology & Biopharmaceutics

Trivedi et al., Clin Pharmacol Biopharm 2015, 4:4
http://dx.doi.org/10.4172/2167-065X.1000145

Research Article Open Access

Physical, Thermal and Spectral Properties of Biofield Energy Treated 2,4-Dihydroxybenzophenone

Mahendra Kumar Trivedi[1], Rama Mohan Tallapragada[1], Alice Branton[1], Dahryn Trivedi[1], Gopal Nayak[1], Rakesh Kumar Mishra[2] and Snehasis Jana[2]*

[1]*Trivedi Global Inc., 10624 S Eastern Avenue Suite A-969, Henderson, NV 89052, USA*
[2]*Trivedi Science Research Laboratory Pvt. Ltd., Hall-A, Chinar Mega Mall, Chinar Fortune City, Hoshangabad Rd., Bhopal- 462026, Madhya Pradesh, India*

Abstract

Study background: 2,4-Dihydroxybenzophenone (DHBP) is an organic compound used for the synthesis of pharmaceutical agents. The objective of this study was to investigate the influence of biofield energy treatment on the physical, thermal and spectral properties of DHBP. The study was performed in two groups (control and treated). The control group remained as untreated, and the treated group received Mr. Trivedi's biofield energy treatment.

Methods: The control and treated DHBP samples were further characterized by X-ray diffraction (XRD), differential scanning calorimetry (DSC), thermogravimetric analysis (TGA), laser particle size analyser, surface area analyser, Fourier transform infrared (FT-IR) spectroscopy, and ultra violet-visible spectroscopy (UV-vis) analysis.

Results: The XRD study indicated a slight decrease in the volume of the unit cell and molecular weight of treated DHBP as compared to the control sample. However, XRD study revealed an increase in average crystallite size of the treated DHBP by 32.73% as compared to the control sample. The DSC characterization showed no significant change in the melting temperature of treated sample. The latent heat of fusion of the treated DHBP was substantially increased by 11.67% as compared to the control. However, TGA analysis showed a decrease in the maximum thermal decomposition temperature (T_{max}) of the treated DHBP (257.66˚C) as compared to the control sample (260.93˚C). The particle size analysis showed a substantial increase in particle size (d_{50} and d_{99}) of the treated DHBP by 41% and 15.8% as compared to the control sample. Additionally, the surface area analysis showed a decrease in surface area by 9.5% in the treated DHBP, which was supported by the particle size results. Nevertheless, FT-IR analysis showed a downward shift of methyl group stretch (2885→2835 cm^{-1}) in the treated sample as compared to the control. The UV analysis showed a blue shift of absorption peak 323→318 nm in the treated sample (T1) as compared to the control.

Conclusion: Altogether, the results showed significant changes in the physical, thermal and spectral properties of treated DHBP as compared to the control.

Keywords: 2,4-Dihydroxybenzophenone; X-ray diffraction; Thermal analysis; Laser particle size analyser; Surface area analyser; Fourier transform infrared spectroscopy; Ultra violet-visible spectroscopy.

Abbreviations: XRD: X-Ray Diffraction; DSC: Differential Scanning Calorimetry; TGA: Thermo Gravimetric Analysis; FTIR: Fourier Transform Infrared Spectroscopy, UV-Vis: Ultra Violet-Visible Spectroscopy Analysis; CAM: Complementary and Alternative Medicine

Introduction

Benzophenone an aromatic ketone is an important class of organic compounds used in perfumes and photochemicals. Benzophenones are used as an intermediate for the synthesis of dyes, pesticides and drugs [1]. These compounds are widely used for the synthesis of various drugs having anxiolytic, hypnotic and antihistaminic activities [2]. 2,4-dihydroxybenzophenone (DHBP) is used as UV-light absorber in resinous and polymer compositions such as polystyrene, acrylonitrile polymer and other copolymers [3]. Moreover, these UV light absorbers are also used in the preparation of sunscreen agents for cosmetic applications. DHBP has been used as promising sunscreen agent that reduces the skin damage by blocking the ultra violet light [2].

The chemical and physical stability of the pharmaceutical compounds are most desired quality attributes that directly affect its safety, efficacy, and shelf life [4]. Hence, it is required to explore some new alternate approaches that could alter the physical and chemical properties of the compounds such as DHBP. Recently biofield energy treatment has been used as a plausible approach for physicochemical modification of metals [5,6], ceramic [7], organic products [8] and pharmaceutical drugs [9]. Therefore, after considering the pharmaceutical applications of DHBP authors planned to investigate the influence of biofield energy treatment on physical, spectral and thermal properties of DHBP.

The National Centre for Complementary and Alternative Medicine (NCCAM), a part of the National Institute of Health (NIH), recommends the use of Complementary and Alternative Medicine (CAM) therapies as an alternative in the healthcare sector, and about 36% of Americans regularly uses some form of CAM [10]. CAM includes numerous energy-healing therapies; biofield therapy is one of the energy medicine used worldwide to improve the health.

Fritz, has first proposed the law of mass-energy interconversion and after that Einstein derived the well-known equation $E=mc^2$ for light and mass [11,12]. Though, conversion of mass into energy is fully

***Corresponding author:** Dr. Snehasis Jana, Trivedi Science Research Laboratory Pvt. Ltd., Hall-A, Chinar Mega Mall, Chinar Fortune City, Hoshangabad Rd., Bhopal- 462026, Madhya Pradesh, India, Tel: +91-755-6660006 E-mail: publication@trivedisrl.com

Received September 08, 2015; **Accepted** September 18, 2015; **Published** September 25, 2015

Citation: Trivedi MK, Tallapragada RM, Branton A, Trivedi D, Nayak G, et al. (2015) Physical, Thermal and Spectral Properties of Biofield Energy Treated 2,4-Dihydroxybenzophenone. Clin Pharmacol Biopharm 4: 145. doi:10.4172/2167-065X.1000145

validated, but the inverse of this relation, *i.e.* energy into mass is not yet verified scientifically. Additionally, it was stated that energy exist in various forms such as kinetic, potential, electrical, magnetic, nuclear, etc. which have been generated from different sources. Similarly, neurons that are present in the human central nervous system have the ability to transmit the information in the form of electrical signals [13-16]. Hence, biofield is defined as a bioenergetic field that permeates and surrounds living organisms. Recently Prakash et al. reported that this inherent biomagnetic field around the human body can be measured by few medical techniques such as Kirlian photography, polycontrast interference photography and resonance field imaging [17].

Therefore, it is envisaged that human beings have the ability to harness the energy from the environment/Universe and can transmit into any object (living or non-living) around the Globe. The object(s) will always receive the energy and responding in a useful manner that is called biofield energy. Mr. Trivedi's unique biofield treatment is also known as The Trivedi Effect®. It is known to transform the characteristics of various living and non-living things. Moreover, the biofield treatment has caused significant affect in different fields such as agriculture [18-20] and microbiology [21-22].

The present work is focused to study the impact of Mr. Trivedi' biofield energy treatment on physical, thermal and spectral properties of DHBP and characterized by XRD, DSC, TGA, particle size, surface area, FT-IR and UV-visible spectroscopic analysis.

Materials and Methods

2,4-Dihydroxybenzophenone (DHBP) was procured from S D Fine Chemicals Ltd, India. The sample was divided into two parts; one was kept as a control sample while the other was subjected to Mr. Trivedi's unique biofield treatment and coded as treated sample. The treated group was in sealed pack and handed over to Mr. Trivedi for biofield energy treatment under standard laboratory conditions. Mr. Trivedi provided the energy treatment through his energy transmission process to the treated group without touching the sample. The control and treated samples were characterized by XRD, DSC, TGA, particle size, surface area, FT-IR, and UV-visible analysis.

Characterization

X-ray diffraction (XRD) study

The XRD analysis of control and treated DHBP was carried out on Phillips, Holland PW 1710 X-ray diffractometer system, which had a copper anode with nickel filter. The radiation of wavelength used by the XRD system was 1.54056 Å. The data obtained from this XRD were in the form of a chart of 2θ *vs.* intensity and a detailed table containing peak intensity counts, d value (Å), peak width (θ°), relative intensity (%) etc. The average crystallite size (G) was calculated by using formula:

$G = k\lambda/(b\text{Cos}\theta)$

Here, λ is the wavelength of radiation used, b is full width half-maximum (FWHM) of peaks and k is the equipment constant (=0.94).

Percent change in unit cell volume = $[(V_t\text{-}V_c)/V_c] \times 100$

The molecular weight of atom was calculated using following equation:

Molecular weight = number of protons x weight of a proton + number of neutrons x weight of a neutron + number of electrons x weight of an electron.

Molecular weight in g/Mol was calculated from the weights of all atoms in a molecule multiplied by the Avogadro number (6.023×10^{23}). The percent change in molecular weight was calculated using the following equation:

Percent change in molecular weight = $[(M_t\text{-}M_c)/M_c] \times 100$

Where, M_c and M_t are molecular weight of control and treated powder sample respectively.

Percentage change in average crystallite size was calculated using following formula:

Percent change in average crystallite size = $[(G_t\text{-}G_c)/G_c] \times 100$

Where, G_c and G_t are the average crystallite size of control and treated powder samples respectively.

Differential scanning calorimetry (DSC)

DSC was used to investigate the melting temperature and latent heat of fusion (ΔH) of samples. The control and treated DHBP samples were analysed using a Pyris-6 Perkin Elmer DSC at a heating rate of 10°C/min under air atmosphere and the air was flushed at a flow rate of 5 mL/min. Predetermined amount of sample was kept in an aluminum pan and closed with a lid. A blank aluminum pan was used as a reference. The percentage change in latent heat of fusion was calculated using following equations:

$$\%\text{ change in Latent heat of fusion} = \frac{[\Delta H_{\text{Treated}} - \Delta H_{\text{Control}}]}{\Delta H_{\text{Control}}} \times 100$$

Where, $\Delta H_{\text{Control}}$ and $\Delta H_{\text{Treated}}$ are the latent heat of fusion of control and treated samples, respectively.

Thermogravimetric analysis-differential thermal analysis (TGA-DTA)

The thermal stability of control and treated DHBP were analyzed by using Mettler Toledo simultaneous TGA and Differential thermal analyser (DTA). The samples were heated from room temperature to 400°C with a heating rate of 5°C/min under air atmosphere.

Particle size analysis

The average particle size and particle size distribution were analyzed by using Sympetac Helos-BF Laser Particle Size Analyser with a detection range of 0.1 to 875 micrometer. Average particle size d_{50} and d_{99} (size exhibited by 99% of powder particles) were computed from laser diffraction data table. The percentage changes in d_{50} and d_{99} values were calculated by the following formula:

Percentage change in d_{50} size = 100 × (d_{50} treated- d_{50} control)/ d_{50} control

Percentage Change in d_{99} size = 100× (d_{99} treated- d_{99} control)/ d_{99} control

Surface area analysis

The surface area of control and treated DHBP were characterized by surface area analyser, SMART SORB 90 Brunauer-Emmett-Teller (BET) using ASTM D 5604 method that had a detection range of 0.2-1000 m^2/g. Percent change in surface area was calculated using following equation:

$$\%\text{ change in surface area} = \frac{[S_{\text{Treated}} - S_{\text{Control}}]}{S_{\text{Control}}} \times 100$$

Where, S_{Control} and S_{Treated} are the surface area of control and treated samples respectively.

FT-IR spectroscopy

The FT-IR spectra were recorded on Shimadzu's Fourier transform infrared spectrometer (Japan) with the frequency range of 4000-500 cm^{-1}. The analysis was accomplished to evaluate the effect of biofield treatment at an atomic level like dipole moment, force constant and bond strength in chemical structure [23]. The treated sample was divided into two parts T1 and T2 for FT-IR analysis.

UV-Vis spectroscopic analysis

UV spectra of the control and treated DHBP samples were recorded on Shimadzu UV-2400 PC series spectrophotometer with 1 cm quartz cell and a slit width of 2.0 nm. The analysis was carried out using wavelength in the range of 200-400 nm and methanol was used as a solvent. The UV spectra was analysed to determine the effect of biofield treatment on the energy gap of highest occupied molecular orbital and lowest unoccupied molecular orbital (HOMO–LUMO gap) [23]. The treated sample was divided in two parts T1 and T2 for the analysis.

Results and Discussion

X-ray diffraction

XRD was used to investigate the crystalline nature of the control and treated DHBP. Figure 1 shows the XRD diffractogram of the control and treated DHBP. XRD diffractogram of the control DHBP showed intense crystalline peaks at 2θ equal to 12.98°, 14.83°, 15.24°, 18.13°, 18.52°, 25.64°, 27.93°, 34.85°, 37.57° and 44.34°. However, the treated DHBP showed XRD peaks at 2θ equal to 12.97°, 14.85°, 15.23°, 18.13°, 18.50°, 25.63°, 27.94°, 34.75°, 34.85°, 37.56°, and 44.34°. The intensity of XRD peaks present at Brags angle 2θ equal to 18.13°, 18.50°, 34.85°, 37.56° and 44.34° were increased in the treated sample as compared to the control. This showed an increase in crystallinity of the treated DHBP with respect to the control sample. It is proposed that biofield energy treatment might increase the long-range order of the DHBP molecules that lead to the formation of the symmetrical crystalline pattern as compared to the untreated sample [24]. Based on XRD peaks, control and treated samples were indexed with the monoclinic crystal structure.

The unit cell volume, crystallite size and change in molecular weight were computed from the XRD diffractogram, and results are presented in Table 1. The unit cell volume of control DHBP was 1063.70 $10^{-24} \times cm^3$ and it was minimally decreased to 1063.20 $10^{-24} \times cm^3$ in the treated sample. The treated DHBP showed a decrease in unit cell volume by 0.05% as compared to the control sample. The molecular weight (number of proton and neutrons) in control DHBP was 214.95 g/mol and it was minimally decreased up to 214.84 g/mol in the treated sample. The treated sample showed 0.048 % change in molecular weight with respect to control. It is hypothesized that biofield energy may be acted on the treated DHBP crystals at nuclear level and altered the number of proton and neutrons as compared to the control, which may lead to change in its molecular weight [25].

The crystallite size is known as a group of molecules or atoms having the same orientation in one plane. Moreover, the crystallite size is one of the crystallographic factors associated with the formation of dislocations and point defects in the crystalline structure, which directly influences the material properties [26]. The crystallite size of the control sample on the plane corresponding to most intense XRD peak (i.e. 2θ = 27.9) was 78.08 nm, and it was remained unchanged in treated DHBP sample (78.08 nm). Nevertheless, the average crystallite size was also calculated from the XRD diffractograms and data are presented in Table 1. The average crystallite size of control DHBP was 62.19 nm, and it was significantly increased to 82.55 nm, in the treated sample. The result showed an increase in average crystallite size by 32.73% in treated sample as compared to the control. Caruntu *et al.* reported that dielectric properties of barium powder could be varied by modulating the crystallite size through an annealing process [27]. Vucinic-Vasic *et al.* during their studies on zinc ferrite nanoparticles revealed that crystallite size increases with elevation in annealing temperature [28]. Additionally, recently it was showed that introduction of ultrasound to materials leads to substantial increase in crystallite size [29]. Hence, it is assumed that biofield treatment may provide waves similar like ultrasound or thermal energy to treated DHBP atoms that led to a decrease in dislocation densities and increase in crystallite size with respect to control.

Thermal analysis

DSC study: DSC was used to investigate the melting point and latent heat of fusion of control and treated DHBP. DSC thermogram of the control and treated DHBP are presented in Figure 2. DSC thermogram of the control DHBP showed a sharp melting endothermic peak at 146.39°C, and it indicated the crystalline nature of the control DHBP. However, the treated DHBP showed a minimal decrease in melting endothermic peak and it was observed at 146.21°C.

The latent heat of fusion of control and treated samples were obtained from respective thermograms and data are presented in

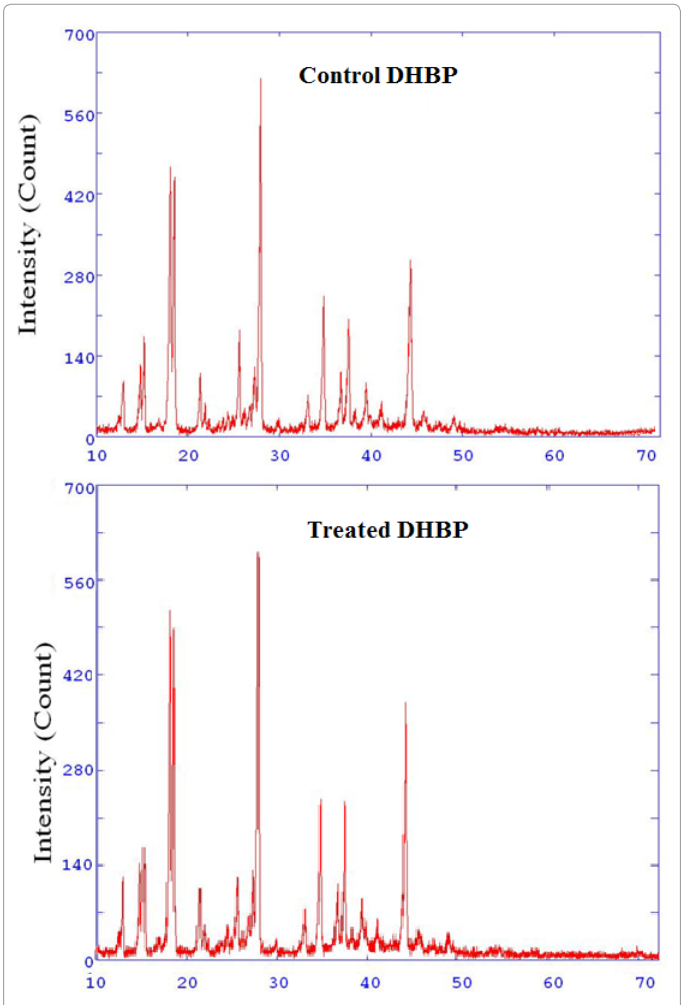

Figure 1: XRD diffractogram of control and treated 2,4-dihydroxybenzophenone.

Compound Characteristics	Control	Treated
Unit cell volume (10^{-24} cm^3)	1063.70	1063.20
Molecular Weight (g/mol)	214.95	214.84
Crystallite size (G' × 10^{-9})	62.19	82.55

Table 1: XRD data (unit cell volume, molecular weight and crystallite size) of control and treated 2,4-dihydroxybenzophenone.

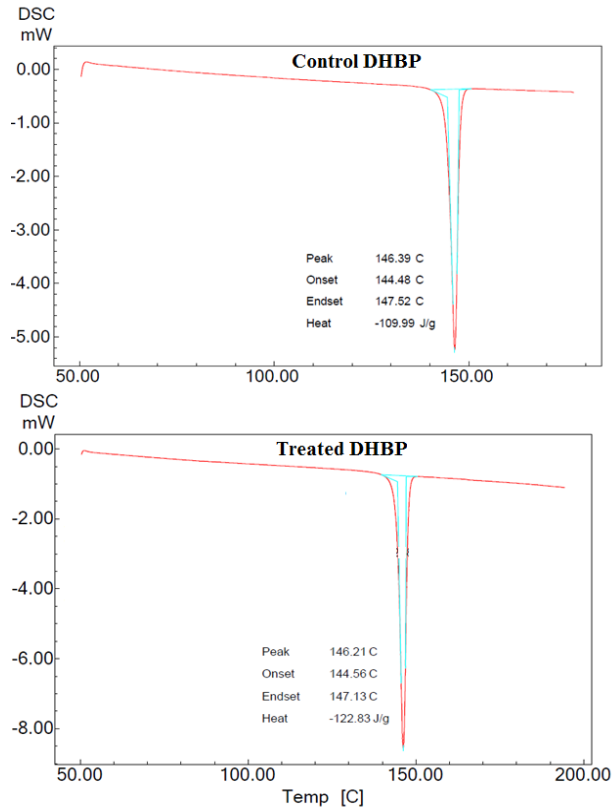

Figure 2: DSC thermogram of control and treated 2,4-dihydroxybenzophenone.

Table 2. The control DHBP showed a latent heat of fusion of 109.99 J/g; however it was increased to 122.83 J/g in the treated DHBP. The latent heat of fusion of DHBP was substantially increased by 11.67% as compared to control. It was suggested that a material consists of strong intermolecular forces that hold them tightly on their positions. The energy needed to overcome the intermolecular force is known as latent heat of fusion. This latent heat of fusion is stored as potential energy in the atoms during its phase transition from solid to liquid [30-31]. It is speculated that biofield treatment may alter the intermolecular force in the sample that leads to increasing in latent heat of fusion of the treated DHBP.

TGA study: TGA was used to evaluate the thermal stability of the control and treated DHBP sample. Figure 3 shows the TGA thermograms of control and treated DHBP. TGA thermogram of control DHBP showed one-step thermal degradation pattern. The control sample started to degrade thermally at around 244°C, and it was terminated at around 285 °C. The control sample lost 55.51% weight during this process. However, the treated DHBP sample started to decompose at around 240°C and stopped at around 282°C. During this thermal process, the treated sample lost 54.89% of its initial weight.

DTA thermogram of the control and treated DHBP are depicted in Figure 3. The DTA of the control DHBP showed an endothermic transition at 144.17°C, which could be associated with melting of the sample. Nevertheless, the treated DHBP showed the same endothermic peak at 143.74°C. This showed the minimal decrease in melting temperature of the treated DHBP as compared to the control. It was previously reported that solid-solid phase transformation with large strain increases the driving force for melting and thus reduces the melting temperature [32]. It is postulated that the biofield energy treatment possibly produced a strain that reduces the melting temperature of the treated DHBP. The temperature at which maximum thermal decomposition (T_{max}) occurred was recorded with derivative thermogravimetry (DTG) and data are presented in Table 2. The control DHBP showed T_{max} at 260.93 °C; however it was decreased to 257.66 °C in treated sample. This indicated the decrease in thermal stability of treated DHBP as compared to the control sample.

Particle size and surface area analysis

The average particle size (d_{50}) and size exhibited by 99% particles (d_{99}) were computed from the particle size distribution curve, and results are presented in Figure 4. The d_{50} of the control DHBP was 64.65 µm and after biofield treatment it was increased substantially to 91.14 µm in the treated DHBP. Whereas, the d_{99} of the control sample was 303.39 µm, and it was increased to 351.40 µm in the treated DHBP. The result showed the substantial increase in d_{50} by 41% in the treated DHBP as compared to the control sample. However, the d_{99} of the treated DHBP was increased by 15.8 % as compared to the control sample. Vinila et al showed that particle size of a ceramic material increases with elevation in temperature [33]. Additionally, Iqbal et al suggested that due to annealing the particles collide and coalesce with one another to form a bigger particle [34]. Hence, it is assumed that biofield treatment may provide some thermal energy that caused aggregation of particles leading to increase in particle size.

The surface area of control and treated DHBP was measured using BET method and data are presented in Figure 5. The surface area of control DHBP was 0.9487 m^2/g and it was decreased to 0.8667 m^2/g, in treated sample. The result indicated the decrease in surface area by 8.64% in treated DHBP as compared to the control sample. It was reported that particle size is inversely proportional to surface area. Thus, increase in particle size causes a decrease in surface area and *vice versa* [35]. This was also supported by the XRD data where average crystallite size of treated sample was increased that causes decrease in the surface area.

FT-IR spectroscopy

FT-IR spectra of control and treated DHBP are shown in Figure 6. The FT-IR spectrum of control DHBP showed –OH stretching vibration peak at 3178 cm^{-1}. However, in the treated DHBP (T1 and T2) the –OH stretching were observed at 3184 and 3180 cm^{-1}, respectively. The aromatic =C-H stretch was assigned at 3064 cm^{-1} in the control and treated samples (T1 and T2). Likewise, the C-H methyl stretch was observed at 2885, 2875 and 2835 cm^{-1} in control and treated samples (T1 and T2), respectively. The aromatic C=C stretching of benzene moiety was appeared in the region of 1597-1627 cm^{-1} in the control and treated samples. The C-H asymmetrical bending peaks were

Parameter	Control	Treated
Latent heat of fusion ΔH (J/g)	109.99	122.83
Melting temperature (°C)	146.39	146.21
T_{max} (°C)	260.93	257.66
Weight loss (%)	55.51	54.89

T_{max}: maximum thermal decomposition temperature

Table 2: Thermal analysis data of control and treated 2,4-dihydroxybenzophenone.

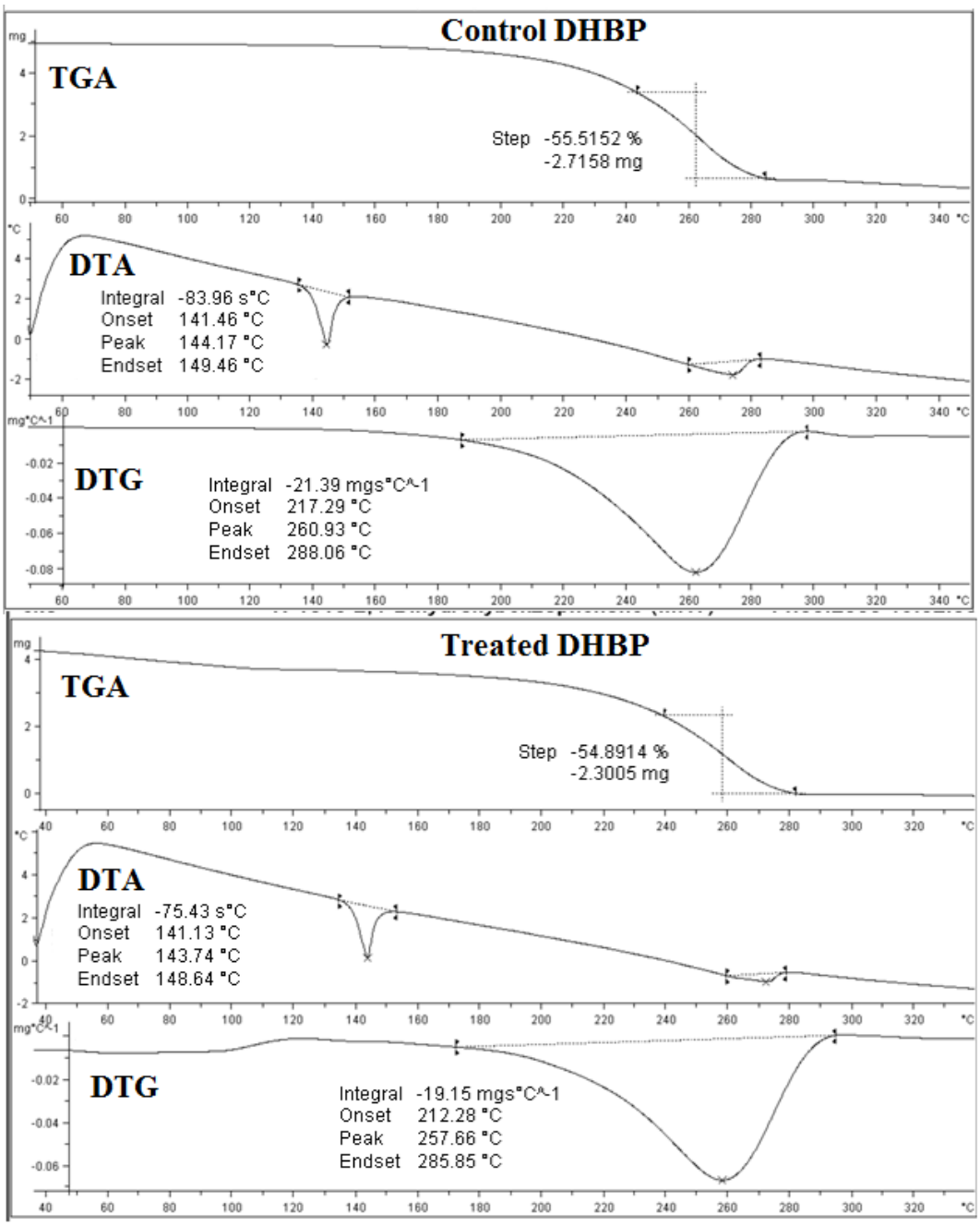

Figure 3: TGA thermogram of control and treated 2,4-dihydroxybenzophenone.

appeared at 1446-1491 cm^{-1} in the control and T1 sample, whereas in the T2 sample these peaks were observed at 1446-1489 cm^{-1}. The C-O stretching for ether linkage was appeared at 1166 cm^{-1} in all the control and the treated samples. The C-H out of plane deformation peaks were observed in the region of 742-850 cm^{-1} in the control sample. However, these peaks were observed in the region of 750-850 cm^{-1} in the treated samples (T1 and T2). Additionally, the C-C stretching was observed at 1280 cm^{-1} in the control and T1 sample; whereas it was appeared at 1290 cm^{-1} in the T2 sample.

Overall, the FT-IR spectra of treated sample showed the downward shift in methyl (C-H) stretch of the treated sample 2885→2835 cm^{-1} as compared to control sample. It was previously suggested that increase in the frequency of any bond causes a possible enhancement in force constant of the respective bond [23]. Hence, it is assumed that biofield energy treatment might alter the dipole moment or force constant of the methyl stretch bond in treated DHBP sample as compared to the control.

UV-visible spectroscopy

UV-visible spectra of control and treated DHBP are shown in Figure 7. The UV spectrum of the control DHBP showed absorption peaks at 204, 242, 289, and 323 nm. The UV spectrum of treated DHBP (T1) showed absorption peaks at 203, 242, 290 and 318 nm. Whereas,

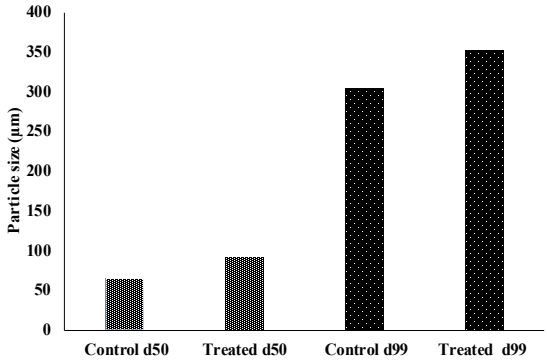

Figure 4: Particle size (d_{50} and d_{99}) of control and treated 2,4-dihydroxybenzophenone.

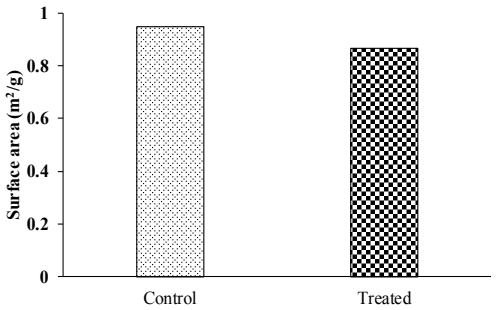

Figure 5: Surface area of control and treated 2,4-dihydroxybenzophenone.

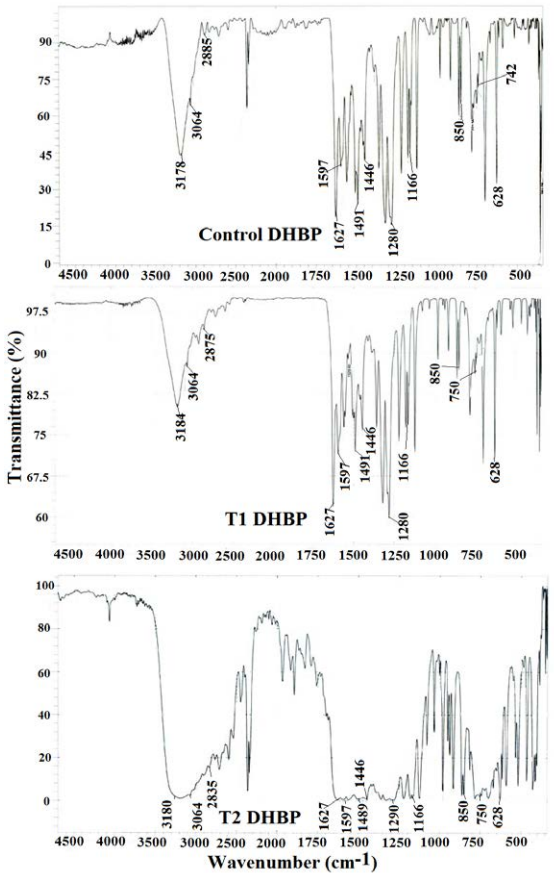

Figure 6: FTIR spectra of control and treated (T1 and T2) 2,4-dihydroxybenzophenone.

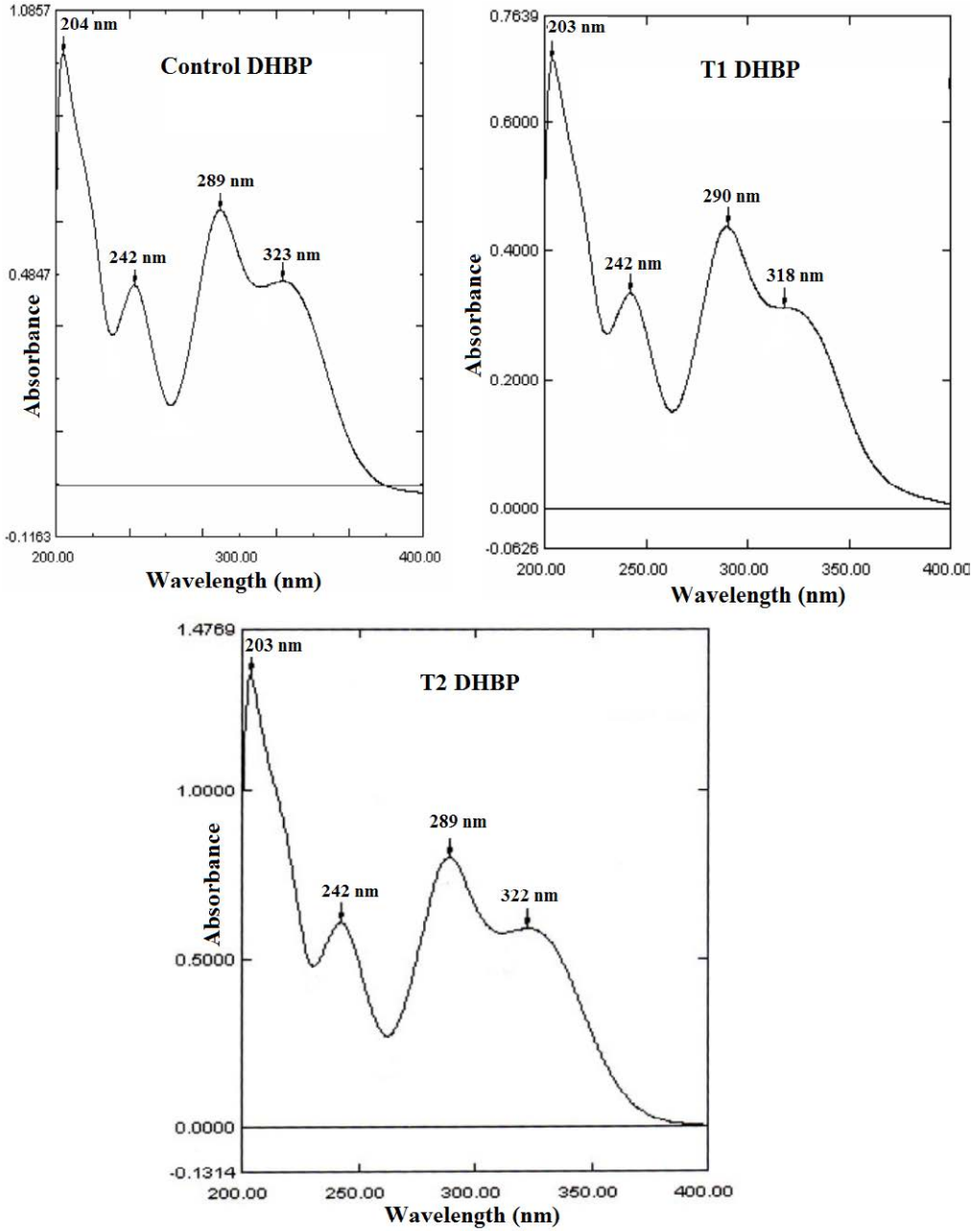

Figure 7: UV visible spectra of control and treated (T1 and T2) 2,4-dihydroxybenzophenone.

the UV spectrum of DHBP (T2) showed absorption peaks at 203, 242, 289 and 322 nm. The result showed a blue shift of absorption peak at 323 nm in the control sample to 318 nm in DHBP sample (T1). It is speculated that the biofield energy treatment may cause changes in the energy gap of highest occupied molecular orbital and lowest unoccupied molecular orbital (HOMO–LUMO gap) of the treated DHBP with respect to the control [23,36].

Conclusions

In summary, the XRD study showed a decrease in the volume of the unit cell and molecular weight of treated DHBP as compared to the control. However, average crystallite size was increased by 32.73% in treated DHBP as compared to the control sample. It is assumed that biofield energy treatment might cause a reduction in dislocation density that lead to an increase in crystallite size in treated sample. The DSC analysis showed an increase in the latent heat of fusion of treated DHBP by 11.67% as compared to the control sample. TGA analysis indicated the decrease in thermal stability of the treated compound as compared to the control. A significant increase by 41% and 15.8% was observed in d_{50} and d_{99}, respectively of the treated DHBP as compared to control sample. Additionally, the BET analysis showed a reduction in surface area (8.64%) of the treated DHBP that was due to increase in particle size of the sample. The UV spectral analysis showed alterations in absorption peak at 323→318 nm in treated sample as compared to the control. Thus, the biofield energy treatment has caused substantial changes in physical, thermal and spectral properties of DHBP.

Acknowledgement

The authors would like to thank all the laboratory staff of MGV Pharmacy College, Nashik for their assistance during the various instrument characterizations. The authors would also like to thank Trivedi Science, Trivedi Master Wellness and Trivedi Testimonials for their support during the work.

References

1. Bezwada RS (2008) Chemistry of benzophenones. Indofine Chemical Company Hillsborough, NJ, USA.
2. Thenmozhi R, Claude A (2012) Rapid crystal growth of benzophenone by low temperature solution growth and its characterization. Archives Appl Sci Res 4: 898-905.
3. Whelen MS (1968) Process for the preparation of 2,4-dihydroxybenzophenone. US 3371119 A.
4. Blessy M, Patel RD, Prajapati PN, Agrawal YK (2014) Development of forced degradation and stability indicating studies of drugs- A review. J Pharm Anal 4: 159-165.
5. Trivedi MK, Patil S, Tallapragada RM (2013) Effect of biofield treatment on the physical and thermal characteristics of silicon, tin and lead powders. J Material Sci Eng 2: 125.
6. Trivedi MK, Patil S, Tallapragada RMR (2015) Effect of biofield treatment on the physical and thermal characteristics of aluminium powders. Ind Eng Manag 4: 151.
7. Trivedi MK, Patil S, Tallapragada RM (2013) Effect of biofield treatment on the physical and thermal characteristics of vanadium pentoxide powder. J Material Sci Eng S11: 001.
8. Trivedi MK, Nayak G, Patil S, Tallapragada RM, Jana S, et al. (2015) Bio-field treatment: An effective strategy to improve the quality of beef extract and meat infusion powder. J Nutr Food Sci 5: 389.
9. Trivedi MK, Patil S, Shettigar H, Bairwa K, Jana S (2015) Effect of biofield treatment on spectral properties of paracetamol and piroxicam. Chem Sci J 6: 98.
10. Barnes PM, Powell-Griner E, McFann K, Nahin RL (2004) Complementary and alternative medicine use among adults: United States, 2002. See comment in PubMed Commons below Adv Data : 1-19.
11. Hasenohrl F (1904) On the theory of radiation in moving bodies. Ann Phys (Berlin) 15: 344-370.
12. Einstein A (1905) Does the inertia of a body depend upon its energy-content? Ann Phys (Berlin) 18: 639-641.
13. Becker RO, Selden G (1985) The body electric: Electromagnetism and the foundation of life. William Morrow and Company, New York City.
14. Born M (1971) The Born-Einstein Letters. (1stedn), Walker and Company, New York.
15. Cohen S1, Popp FA (2003) Biophoton emission of human body. See comment in PubMed Commons below Indian J Exp Biol 41: 440-445.
16. BARNES RB (1963) Thermography of the human body. See comment in PubMed Commons below Science 140: 870-877.
17. Prakash S, Chowdhury AR, Gupta A (2015) Monitoring the human health by measuring the biofield “aura”: An overview. IJAER 10: 27637-27641.
18. Shinde V, Sances F, Patil S, Spence A (2012) Impact of biofield treatment on growth and yield of lettuce and tomato. Aust J Basic Appl Sci 6: 100-105.
19. Sances F, Flora E, Patil S, Spence A, Shinde V (2013) Impact of biofield treatment on ginseng and organic blueberry yield. Agrivita J Agric Sci 35: 22-29.
20. Patil SA, Nayak GB, Barve SS, Tembe RP, Khan RR (2012) Impact of biofield treatment on growth and anatomical characteristics of Pogostemon cablin (Benth.). Biotechnology 11: 154-162.
21. Trivedi MK, Patil S, Shettigar H, Bairwa K, Jana S (2015) Phenotypic and biotypic characterization of Klebsiella oxytoca: An impact of biofield treatment. J Microb Biochem Technol 7: 203-206.
22. Trivedi MK, Patil S, Shettigar H, Gangwar M, Jana S (2015) An effect of biofield treatment on multidrug-resistant Burkholderia cepacia: A multihost pathogen. J Trop Dis 3: 167.
23. Pavia DL, Lampman GM, Kriz GS (2001) Introduction to spectroscopy. (3rdedn), Thomson Learning, Singapore.
24. Pavlov VV (2008) Distinctive features of a crystal, Ñ Crystal-like properties of a liquid and atomic quantum effects. JPCS 98: 052008.
25. Trivedi MK, Nayak G, Patil S, Tallapragada RM, Latiyal O (2015) Studies of the atomic and crystalline characteristics of ceramic oxide nano powders after bio field treatment. Ind Eng Manage 4: 161.
26. Ohira T, Yamamoto O (2012) Correlation between antibacterial activity and crystallite size on ceramics. Chem Eng Sci 68: 355-361.
27. Caruntu G, Rarig Jr R, Dumitru I, O’Connor CJ (2006) Annealing effects on the crystallite size and dielectric properties of ultrafine Ba1-x SrxTiO3 powders synthesized through an oxalate-complex precursor. J Mater Chem 16: 752-758.
28. Vucinic-Vasic M, Bozin ES, Bessais L, Stojanovic G, Kozmidis-Luburic U (2013) Thermal evolution of cation distribution/crystallite size and their correlation with the magnetic state of Yb-substituted zinc ferrite nanoparticles. J Phys Chem C 117: 12358-12365.
29. Cherepanov PV1, Melnyk I2, Andreeva DV2 (2015) Effect of high intensity ultrasound on Alâ‚ƒNiâ‚„ Alâ‚ƒNi crystallite size in binary AlNi (50 wt% of Ni) alloy. See comment in PubMed Commons below Ultrason Sonochem 23: 26-30.
30. Moore J (2010) Chemistry: The molecular science (4thedn), Brooks Cole.
31. Trivedi MK, Tallapragada RM, Branton A, Trivedi A, Nayak G, et al. (2015) Biofield Treatment: A potential strategy for modification of physical and thermal properties of indole. J Environ Anal Chem 2: 152.
32. Levitas VI, Henson BF, Smilowitz LB, Asay BW (2006) Solid-solid phase transformation via internal stress-induced virtual melting, significantly below the melting temperature. Application to HMX energetic crystal. J Phys Chem B 110: 10105-10119.
33. Vinila VS, Reenu J, Mony A, Nair HG, Issac S (2014) XRD studies on nano crystalline ceramic superconductor PbSrCaCuO at different treating temperatures. Crystal Struct Theory Appl 3: 1-9.
34. Iqbal MZ, Ali S, Mirza MA (2008) Effect of particle size on the structural and transport properties. JNSMAC 48: 51-63.
35. Khadka P, Ro J, Kim H, Kim I, Kim JT, et al. (2014) Pharmaceutical particle technologies: An approach to improve drug solubility, dissolution and bioavailability. Asian J Pharm Sci 9: 304 -316.
36. Pudlak M, Pincak R (2009) Energy gap between highest occupied molecular orbital and lowest unoccupied molecular orbital in multiwalled fullerenes. Phys Rev 79: 033202.

Citation: Trivedi MK, Tallapragada RM, Branton A, Trivedi D, Nayak G, et al. (2015) Physical, Thermal and Spectral Properties of Biofield Energy Treated 2,4-Dihydroxybenzophenone. Clin Pharmacol Biopharm 4: 145. doi:10.4172/2167-065X.1000145